BBA - Molecular Basis of Disease 1865 (2019) 2303–2316

Contents lists available at ScienceDirect

BBA - Molecular Basis of Disease

journal homepage: www.elsevier.com/locate/bbadis

Hemin-induced platelet activation and ferroptosis is mediated through ROS-driven proteasomal activity and inflammasome activation: Protection by Melatonin

Somanathapura K. NaveenKumar[a], Mahadevappa Hemshekhar[a,b], Kempaiah Kemparaju[a,*], Kesturu S. Girish[a,c,**]

[a] DOS in Biochemistry, University of Mysore, Manasagangotri, Mysuru 570 006, India
[b] Department of Internal Medicine, Manitoba Centre for Proteomics and Systems Biology, University of Manitoba, Winnipeg, MB R3E 3P4, Canada
[c] Department of Studies and Research in Biochemistry, Tumkur University, Tumakuru 572 103, India

ARTICLE INFO

Keywords:
ROS
Platelets activation
Ferroptosis
Proteasome
Inflammasome
Melatonin

ABSTRACT

Reactive oxygen species (ROS) are capable of inducing cell death or apoptosis. Recently, we demonstrated that lipid-ROS can mediate ferroptosis and activation of human platelets. Ferroptosis is an intracellular iron-mediated cell death, distinct from classical apoptosis and necrosis, which is mediated through the accumulation of ROS, lipid peroxides and depletion of cellular GSH. Lately, we demonstrated that hemoglobin degradation product hemin induces ferroptosis in platelets *via* ROS and lipid peroxidation. In this study, we demonstrate that hemin-induced ferroptosis in platelets is mediated through ROS-driven proteasome activity and inflammasome activation, which were mitigated by Melatonin (MLT). Although inflammasome activation is linked with pyroptosis, it is still not clear whether ferroptosis is associated with inflammasome activation. Our study for the first time demonstrates an association of platelet activation/ferroptosis with proteasome activity and inflammasome activation. Although, high-throughput screening has recognized ferrostatin-1 (Fer-1) and liproxstatin-1 (Lip-1) as potent ferroptosis inhibitors, having an endogenous antioxidant such as MLT as ferroptosis inhibitor is of high interest. MLT is a well-known chronobiotic hormone that regulates the circadian rhythms in vertebrates. It also exhibits potent antioxidant and ROS quenching capabilities. MLT can regulate fundamental cellular functions by exhibiting cytoprotective, oncostatic, antiaging, anti-venom, and immunomodulatory activities. The ROS scavenging capacity of MLT is key for its cytoprotective and anti-apoptotic properties. Considering the anti-ferroptotic and anti-apoptotic potentials of MLT, it could be a promising clinical application to treat hemolytic, thrombotic and thrombocytopenic conditions. Therefore, we propose MLT as a pharmacological and therapeutic agent to inhibit ferroptosis and platelet activation.

1. Introduction

Free radicals play a key role in cellular homeostasis and cell cycle [1]. Increased levels of free radicals are shown to interfere in the fundamental cellular functions and survival [1]. Free radicals such as Reactive oxygen species (ROS) are capable of inducing cell death or apoptosis [2]. Recently, we demonstrated that ROS mediate ferroptosis and activation of human platelets. Ferroptosis is intracellular iron-mediated cell death, which is morphologically, biochemically, and genetically distinct from apoptosis and necrosis [3,4]. It is independent of caspase activation, however, ferroptosis is mediated through the accumulation of ROS, lipid peroxides and depletion of cellular GSH. Lately, several studies reported close associations of ferroptosis with various human diseases, including Huntington's disease (HD) [5], periventricular leukomalacia (PVL) [6], hemolytic disorders [4] and renal dysfunction [6].

Ferroptosis can be induced by several small molecules like erastin, SAS and RSL3 [7–9]. Recently we demonstrated that hemoglobin degradation product hemin can induce ferroptosis in platelets *via* ROS and lipid peroxidation [4]. In this study, we demonstrate that hemin induces ferroptosis in platelets by modulating proteasome activity and inflammasome activation and MLT effectively inhibits hemin induced ferroptosis in platelets by restoring proteasome activity and inhibiting inflammasome activation. Although, inflammasome activation is linked

* Correspondence to: K. Kemparaju, Department of Studies in Biochemistry, University of Mysore, Mysuru 570 006, India.
** Correspondence to: K. S. Girish, Department of Studies and Research in Biochemistry, Tumkur University, Tumakuru, 572 103, India.
E-mail addresses: kemparajuom@gmail.com (K. Kemparaju), ksgbaboo@gmail.com (K.S. Girish).

https://doi.org/10.1016/j.bbadis.2019.05.009
Received 20 February 2019; Received in revised form 10 May 2019; Accepted 13 May 2019
Available online 16 May 2019
0925-4439/

with pyroptosis [10], it is still not clear whether ferroptosis is associated with inflammasome activation. It is interesting to discover the association of proteasome activity, inflammasome activation and ferroptosis, particularly in platelets. Platelets being anuclear, possess necessary proteins to undergo apoptosis and ferroptosis [11,12]. High-throughput screening has recognized ferrostatin-1 (Fer-1) and liproxstatin-1 (Lip-1) as potent ferroptosis inhibitors [13]. Both Fer-1 and Lip-1 radical-trapping antioxidants that scavenge peroxide and hydroxide radicals, however, having an endogenous antioxidant as ferroptosis inhibitor is of high interest.

Melatonin (MLT) is a chronobiotic hormone that tightly regulates the circadian rhythms setting a biological clock in vertebrates [14,15]. However, MLT is also known to regulate fundamental cellular functions by exhibiting antioxidant, antiaging, antivenom, oncostatic, cytoprotective and immunomodulatory activities [14–20]. The ability of MLT to scavenge ROS is vital for its cytoprotective and anti-apoptotic properties [17,21,22]. The demonstrated pharmacological abilities of MLT reflect its potential clinical relevance. MLT being an antioxidant scavenges free radicals to suppress oxidative stress and cellular damage by regulating endogenous redox system and key signalling cascades [23,24]. The cytoprotective ability of MLT on various cell types is highly recognized [17,25], however, it exhibits a biphasic behavior by inducing apoptosis at higher doses [26–28].

In this study, we demonstrate that hemin-induces ferroptosis and platelet activation through ROS-mediated proteasomal activity and inflammasome activation, and MLT effectively counteracts. Therefore, we propose MLT as a ferroptosis and platelet activation inhibitor that can be high pharmacological and therapeutic agent to treat thrombotic and thrombocytopenic conditions.

2. Materials and methods

2.1. Materials

Hemin, ferrostatin-1 (FS-1), monochlorobimane (MCB), thrombin from bovine plasma, calcium ionophore (A23187), Mouse sP-Selectin ELISA Kit (RAB0427 SIGMA), Suc-Leu-Leu-Val-Tyr-AMC (fluorogenic proteasome substrate) and 10-nonyl acridine orange (NAO) were purchased from Sigma Chemicals, USA. Deferoxamine (DFO) was purchased from Novartis India Ltd. Tin protoporphyrin IX dichloride (SnPP), ABT-737, calcein-AM and BAX, BAK, Bcl-2, Bcl-xL, BID and were obtained from Santa Cruz Biotechnology, Inc., USA. Antibodies against ubiquitinated proteins, COX-IV and β-tubulin were purchased from Cell Signalling and Technology, USA. FITC conjugated CD41 and FITC-conjugated CD62P (P-selectin) were purchased from BD Biosciences, USA. Alexa Fluor-546 Phalloidin, DCFDA, and BODIPY 581/591 C11 were purchased from Molecular Probes, Thermo Fisher Scientific, USA. LDH estimation kits were purchased from Agappe Diagnostics Limited, India. Hydrogen peroxide (H_2O_2) was from RANKEM, India. Melatonin (MLT) and all other chemicals were of analytical grade and purchased from Sisco Research Laboratories, Mumbai, India. Melatonin was dissolved in DMSO and diluted in Tyrode's buffer and the amount of DMSO in the reaction was maintained < 1%. For *in vivo* experiments MLT was dissolved in absolute ethanol and diluted in phosphate-buffered saline (PBS) and the amount of ethanol maintained < 1%.

2.2. Preparation of platelets

Blood was collected from healthy human volunteers with informed consent according to the approved guidelines of Institutional Human Ethical Committee (IHEC-UOM No. 114 Ph.D/2015–16), University of Mysore, Mysuru. Blood was drawn from an antecubital vein and was immediately mixed with acid citrate dextrose (ACD) anti-coagulant and platelets were isolated as described previously. Briefly, human platelet-rich plasma was prepared by centrifuging anticoagulated blood at 150 ×*g* for 15 min and the supernatant was collected and centrifuged at 700 ×*g* for 10 min at 37 °C. The platelet pellet was washed twice by suspending them in CGS (13 mM trisodium citrate, 33 mM D-glucose, 123 mM NaCl, pH 6.5) buffer and centrifuged at 700 ×*g* for 15 min at 37 °C. Finally, the washed platelets (WPs) were suspended in Tyrode's buffer (2.5 mM HEPES, 150 mM NaCl, 2.5 mM KCl, 12 mM NaHCO3, 1 mM CaCl2, 1 mM MgCl2, 5.5 mM D-glucose, pH 7.4). The cell count was determined in WPs suspension using a Neubauer chamber and adjusted to 2×10^7 platelets/mL in the final suspension using Tyrode's buffer [4,11].

2.3. Mice

Male Swiss albino mice (8- to 10-weeks old) weighing 20–25 g was obtained from the Central Animal House Facility, Department of Zoology, University of Mysore, Mysuru, India. The animal experiments were approved by the Institutional Animal Ethical Committee, University of Mysore, Mysuru (Approval numbers: UOM/IAEC/23/2011 dated 03-07-2016). Mice were divided into three groups each having 5 mice ($n = 5$). Group I; vehicle control, Group II; Hemin (50 μmol/kg body weight i.p.) [29,30], Group III; Hemin (50 μmol/kg body weight) + MLT (20 mg/kg body weight). Hemin (50 μmol/kg body weight) (i.p.) was injected every 24 h for 3 days (72 h) and a group of mice received MLT (20 mg/kg body weight) (i.p.), after 2 h of every hemin injection. At the end of the 72 h after hemin or MLT treatments, animals were euthanized and blood was collected immediately through cardiac puncture. About 1/4 fraction of the blood was used to separate serum and the remaining blood was immediately mixed with ACD and was then centrifuged to obtain plasma from which platelets were isolated. The cell count was determined in platelets suspension using a Neubauer chamber and adjusted to 4×10^8 cells/mL in the final suspension using Tyrode's buffer/HBSS. Further, isolated platelets were used to determine oxidative stress markers using specific probes and analyzed using a multimode plate reader (microplate reader, TECAN, Switzerland). Lungs and kidney tissues from experimental animals were harvested and rinsed in ice-cold saline and kept in formalin for histological analysis. Serum was separated and stored at −80 °C for further analysis [11].

2.4. Evaluation of platelets viability by MTT assay

MTT colorimetric assay was performed to assess the platelet viability. Washed platelets (1×10^6 cells/mL) were taken separately in 96-well microtiter plates and depending on the desired conditions, treated with hemin (0–25 μM), MLT (1 to 10 μM), DFO (100 μM), FS-1 (5 μM), β-ME (50 μM), cystine (250 μM), SnPP (10 μM), MCC950 (10 μM) and luzindole (25 μM), the final volume was made up to 200 μL using Tyrode's buffer and incubated for 30 min at 37 °C. ABT-373 (5 μM) was taken as positive control. After 1 h of incubation, 250 μM of MTT (3-(4,5-dimethylthiazol-2-yl)-2,5-diphenyltetrazolium bromide) was added and incubated for additional 3 h. Thereafter, MTT was removed and remaining formazan crystals were completely dissolved in DMSO and the absorbance was recorded at 570 nm using a Varioskan multimode plate reader (Thermo Scientific, USA) [4,11].

2.5. Measurement of LDH leakage

Platelets (4×10^6 cells/mL) were treated with hemin (0–25 μM) in presence and absences of MLT (5 to 10 μM) DFO (100 μM) and FS-1 (5 μM). A23187 (5 μM) for 30 min at 37 °C was used as positive control and platelets were pelleted by centrifugation at 3700 ×*g* for 10 min. The supernatant was collected and used to detect LDH release using LDH kit, according to the manufacturer's protocol. The assay was performed in a time course of decrease in NADH absorbance at 340 nm for 3 min [4].

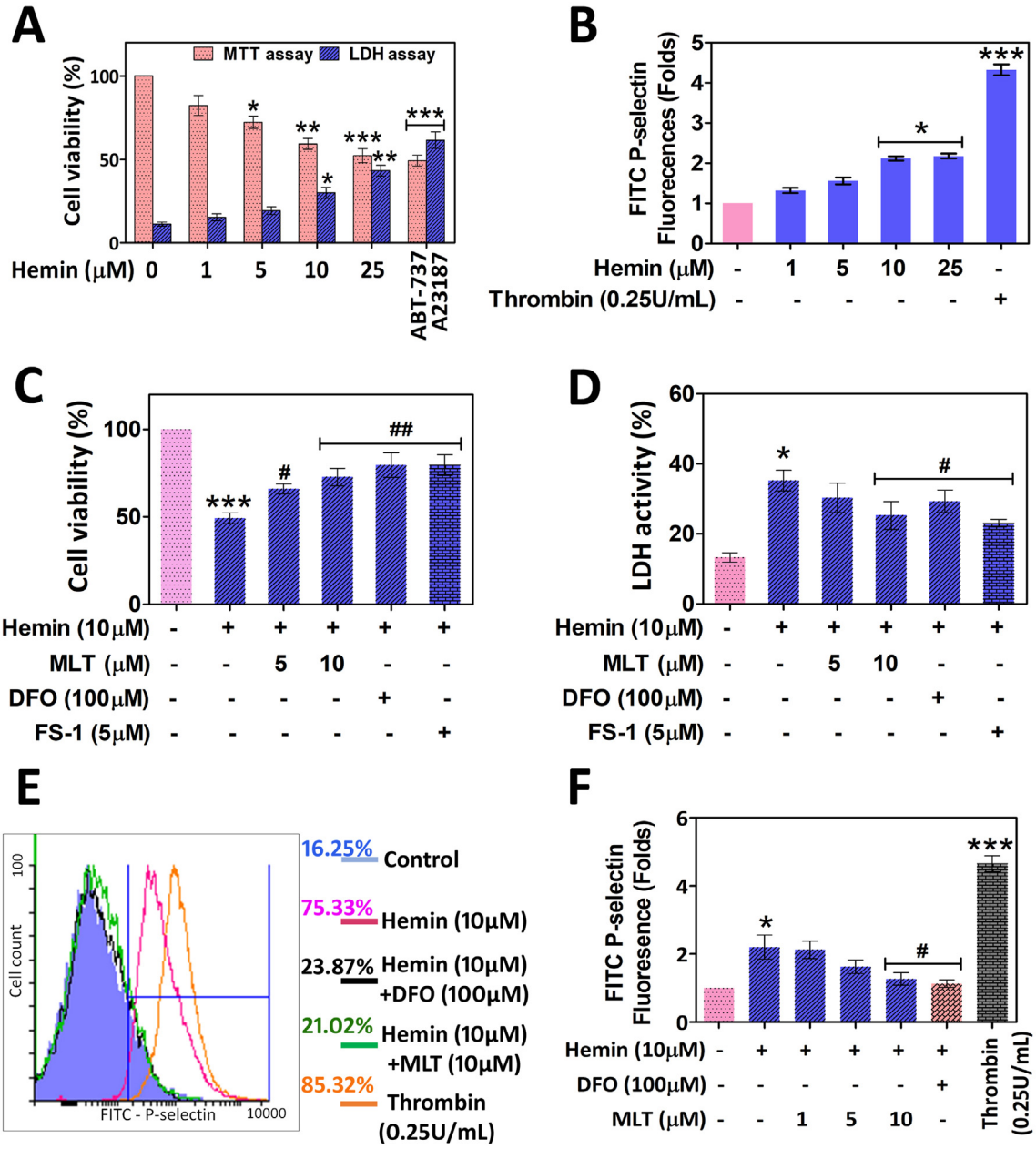

Fig. 1. Hemin-induced platelet activation and death is inhibited by MLT. (A) Dose-dependent effect of hemin (1 to 25 μM) on platelet viability evaluated by MTT and LDH assays. (B) FACS analysis of surface P-selectin expression using FITC-conjugated CD62P in dose-dependent hemin-treated platelets (1 to 25 μM). (C and D) Assessment of platelet viability by MTT assay and LDH release assay in hemin (10 μM)-treated platelets in presence or absences of different doses of MLT (5 to 10 μM), DFO: intracellular iron chelator and FS-1: a ferroptosis inhibitor. (E and F) FACS analysis of P-selectin expression in hemin-treated platelets in the presence or absence of MLT (1 to 10 μM) and DFO (100 μM). ABT-737 (anti-apoptotic Bcl-2 family protein inhibitor), A23187 (calcium ionophore) and thrombin (0.25 U/mL) were used as positive controls. The data is presented as mean ± SEM ($n = 5$) and analyzed using one-way ANOVA followed by Bonferroni posttests, $p^{*}/^{\#} < 0.05$, $p^{**}/^{\#\#} < 0.01$, $p^{***}/^{\#\#\#} < 0.001$; *significant compared to untreated platelets; #significant compared to hemin (10 μM) alone treated platelets.

2.6. Flow cytometric analysis

To assess cellular ROS level, mitochondrial membrane potential, cardiolipin oxidation, cellular GSH level and lipid peroxidation level in platelet suspension (5×10^6 cells) was treated with either Hemin (0–25 μM), MLT (1–10 μM), DFO (100 μM), FS-1 (5 μM), MCC950 (10 μM) and luzindole (25 μM), and incubated for 30 min at 37 °C. After incubation platelets were washed with Tyrode's buffer and incubated with CMDCFDA (5 μM), JC-1 (5 μM), NAO (2 μM), MCB (5 μM) and BODIPY (1 μM) for 30 min at 37 °C in dark. Platelets treated with H_2O_2, A23187, and ABT-737 for 15 min were used as positive control. Cells were again washed, and fluorescence was analyzed using flow cytometry (BD FACSCelesta™) [4,11,31].

2.7. Quantification of total reactive oxygen species (ROS) using DCFDA

To assess whether the hemin induces an increase in the intracellular ROS level, platelet in suspension (5×10^6 cells) were treated with increased concentration of hemin (1 to 25 μM) in presence or absence of MLT (1–10 μM), DFO (100 μM), β-ME (50 μM) and cystine (250 μM) and incubated for 30 min at 37 °C, after incubation platelets were washed with Tyrode's buffer and incubated with CMDCFDA (5 μM) for 30 min at 37 °C in dark. Platelets treated with H_2O_2 (50 μM) for 15 min incubation was used as positive control. Cells were again washed, and

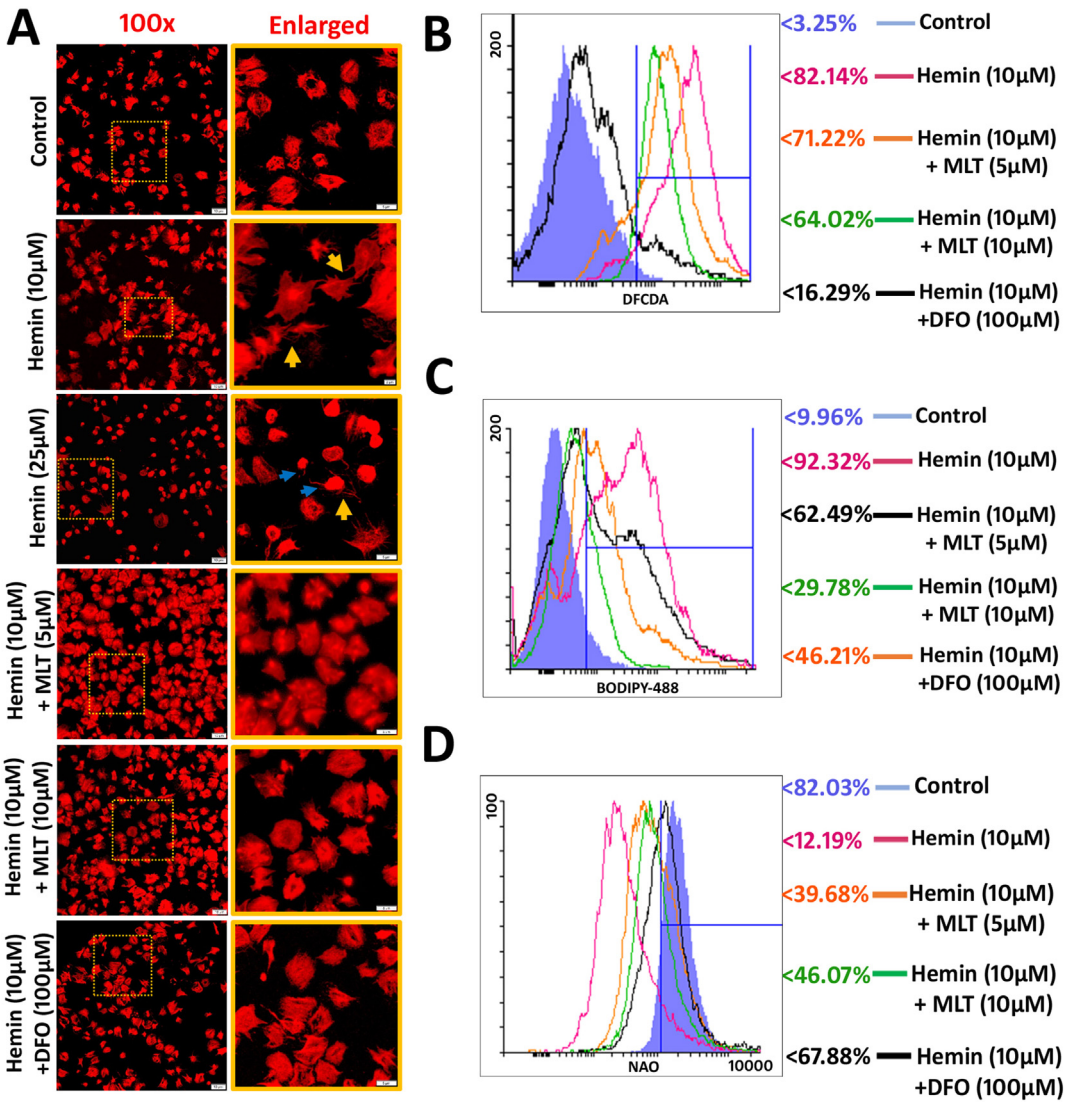

Fig. 2. Hemin-induced actin dynamics, lipid peroxidation, and cardiolipin oxidation are mitigated by MLT. (A) Confocal microscopic evaluation of F-actin dynamics in hemin-treated platelets using Phalloidin-Alexa-546 with enlarged images, yellow arrows indicate the formation of filopodia and lamellipodia and blue arrows indicate destroyed filopodia-like structures. (B) FACS analysis of ROS generation in hemin-treated platelets using DCFDA, (C) lipid peroxide generation using BODIPY-C11 and (D) cardiolipin oxidation using NAO in presence and absence of MLT (5–10 μM) and DFO (100 μM).

fluorescence was analyzed using flow cytometry (BD FACSCelesta) [4,11].

2.8. Quantification of lipid peroxidation using BODIPY 581/591 C11

We examined the hemin-treated platelets for lipid peroxidation using C11-BODIPY 591/581 fluorescent dye which potentially probes the lipid peroxidation level in live cells. Platelet (5×10^6 cells) were treated with various concentration of hemin (1 to 10 μM) in presence and absence of MLT (1–10 μM) and DFO (100 μM) incubated for 30 min at 37 °C and then incubated with BODIPY 581/591 C11 (10 μM) for 20 min at 37 °C in dark. Platelets were again washed, and fluorescence was analyzed using flow cytometry (BD FACSCelesta) [4].

2.9. FACS analysis of P-selectin expression in hemin-treated platelets

To assess whether hemin induces platelet activation, platelet suspension (5×10^6 cells) were treated with concentration-dependent hemin (10 μM) in presence or absence of MLT (1 to 10 μM), DFO (100 μM), MCC950 (10 μM) and luzindole (25 μM), and incubated for 30 min at 37 °C. After incubation, cells were treated with FITC conjugated human P-selectin (2 μL) for 15 min at the room before fixing with 2% paraformaldehyde for 15 mins in dark. Platelets were then washed, and fluorescence was measured using flow cytometry (BD FACSCelesta) [4].

2.10. Confocal microscopic study of actin dynamics in hemin-treated platelets

During platelet activation and death, cytoskeleton actin reorganizes which transforms it into a spiky dynamic and small fragment. To evaluate the actin dynamics in hemin-treated platelets, we performed a confocal microscopy using Alexa-546 conjugated Phalloidin for cytoskeleton actin. Platelets (5×10^6 cells) were treated with concentration-dependent hemin (10 to 25 μM) in presence or absence of MLT (5 to 10 μM) and DFO (100 μM) incubation for 30 min at 37 °C. After incubation, treated platelets were allowed to settle on fibrinogen-coated coverslips for 30 min, followed by incubation, platelets were fixed and permeabilized for 10 min using 0.5% triton-X 100 in PBS with 2% BSA, and then incubated with Alexa-546 conjugated Phalloidin for 2 h. Platelets were then washed, mounted and images were acquired on a FLUOVIEW FV3000, Confocal Laser Scanning Microscope (Olympus,

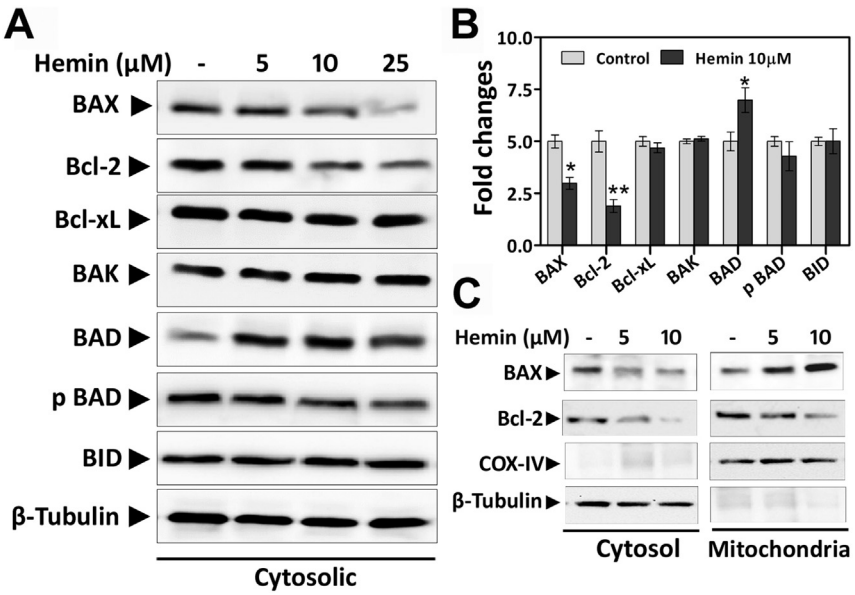

Fig. 3. Hemin-induced altered expression of Bcl-2 family proteins. (A) Immunoblots of Bcl-2 family proteins (BAX, Bcl-2, Bcl-xL, BAK, BAD, phosphoBAD and BID) in hemin-treated platelets, (B) Representative densitogram of immunoblots present in panel A after normalization with respective loading controls. (C) Expression of BAX and Bcl-2 in both mitochondria and cytosolic fractions of hemin-treated platelets. COX-IV (cytochrome *c* oxidase subunit-IV) used as mitochondrial loading control and β-tubulin as a loading control for cytosolic fractions. Data is presented as mean ± SEM ($n = 5$), $p^* < 0.05$, $p^{**} < 0.01$, $p^{***} < 0.001$; *significant compared to control platelets.

Japan). Images were analyzed using the FV31S-DT software [32].

2.11. Proteasome activity assay

Platelets were incubated at 37 °C for 30 min with hemin (1 to 25 μM) in presence or absence of MLT (5 to 10 μM), DFO (100 μM), SnPP (10 μM) and washed twice in Tyrode's buffer. MG-132 (25 μM) was used as positive control for cellular proteasome inhibition. Cells were pelleted and resuspended in permeabilization buffer (20 mM HEPES, 0.2% Triton X-100, 300 mM NaCl and 2 mM EGTA, pH 7.7) followed by addition of 26 proteasome assay buffer (40 mM HEPES, 1 mM EDTA and 0.07% SDS, pH 7.8). Permeabilized cells were added to the 96 well microplates and incubated at 37 °C. The reaction was started by the addition of Suc-Leu-Leu-Val-Tyr-AMC (25 mM) in DMSO and was monitored for 10 min (excitation, 360 nm; emission, 460 nm). Proteasome peptidase activities were determined from SucLLVY-AMC-hydrolyzing activity (chymotrypsin-like activity) [33,34].

2.12. Estimation of glutathione (GSH) level

Platelets (5×10^6 cells/mL) were treated with hemin (1 to 25 μM) in presence or absence of MLT (5 to 10 μM), DFO (100 μM) and incubated for 30 mins at 37 °C. H_2O_2 (10 μM) was used as positive control. After incubation, platelets were incubated with *o*-phthalaldehyde (1 mg/mL) at room temperature for 15 min to determine GSH levels and to determine GSSG, platelets were treated with *N*-ethylmaleimide (10 μM) prior to *o*-phthalaldehyde treatment and the resulting fluorescence was measured at 365 nm excitation and 430 nm emission wavelengths using a Varioskan multimode plate reader (Thermo Scientific, USA). The concentration of GSH and GSSG were determined from the standard curve [4].

2.13. Determination of cellular GSH using monochlorobimane (MCB) by confocal microscopy

Platelets (4×10^8 cells/mL) were treated with hemin (1 to 25 μM) in presence or absence of MLT (5 to 10 μM), DFO (100 μM), SnPP (10 μM) and incubated for 30 min at 37 °C. After incubation, the treated platelets were allowed to settle on fibrinogen-coated coverslips for 30 min, followed by incubation with MCB (5 μM) for 30–45 min before fixing with 2% paraformaldehyde for 15 min. After fixation platelets were stained with CD41 using FITC conjugated CD41 for 2 h at RT. Platelets were then washed, mounted and images were acquired on a FLUOVIEW FV3000, Confocal Laser Scanning Microscope (Olympus, Japan). Images were analyzed using the FV31S-DT software [4].

2.14. Immunoblotting

Platelet lysates and serum samples of treated groups were used for immunoblotting analysis. Platelets (4×10^8 platelets/mL) treated with hemin (10 μM), or MLT (5 to 10 μM), DFO (100 μM), FS-1 (5 μM), MCC950 (10 μM) and luzindole (25 μM) were lysed using lysis buffer (50 mM Tris-HCl, pH 8, containing 1% NP-40, 150 mM NaCl along with protease inhibitor cocktail). The protein concentration was estimated by using the Bradford method and equal amounts of protein (50 μg) were electrophoretically resolved on 10% SDS-PAGE and transferred onto a PVDF membrane. Membranes were blocked with 5% skimmed milk in TBST for 1 h and were incubated overnight with primary antibody against ubiquitin proteins, BAX, Bcl-2, Bcl-xL, BAK, BAD, pBAD, BID, COX-IV, anti-ubiquitinated protein, TNF-α, IL-6, IL-1β, IL-23, IL-10 and β-Tubulin at 4 °C. Membranes were then incubated with appropriate horseradish peroxidase (HRP)-conjugated secondary antibody and developed by enhanced chemiluminescence imaging system (Alliance 2.7, Uvitec, UK) [11,31].

2.15. Determination and quantification of plasma sP-selectin levels

Cell-free plasma samples from treated or untreated mice were used to quantify the soluble P-selectin levels by mouse sP-selectin ELISA kit (RAB0427, Sigma) according to manufacturer's instructions.

2.16. Measurement of γ-glutamyltransferase (GGT) activity

GGT plays a key role in the γ-glutamyl cycle, a critical pathway for glutathione homeostasis. To determine the GGT activity, platelets (5×10^6 cells/mL) isolated from treated mice blood and lysed using distilled water or by sonication. The resulting lysate was used to determine GGT activity. The activity was monitored in 1 mL reaction volume consisting of γ-glutamyl-p-nitroanilide (4 mM), glycylglycine (40 mM) in Tris-HCl buffer (185 mM, pH 8.2). The results were calculated using molar extinction coefficient for p-nitroanilide ($9900\ M^{-1}\ cm^{-1}$) at 405 nm expressed as mM p-nitroanilide formed/min/mg protein [11].

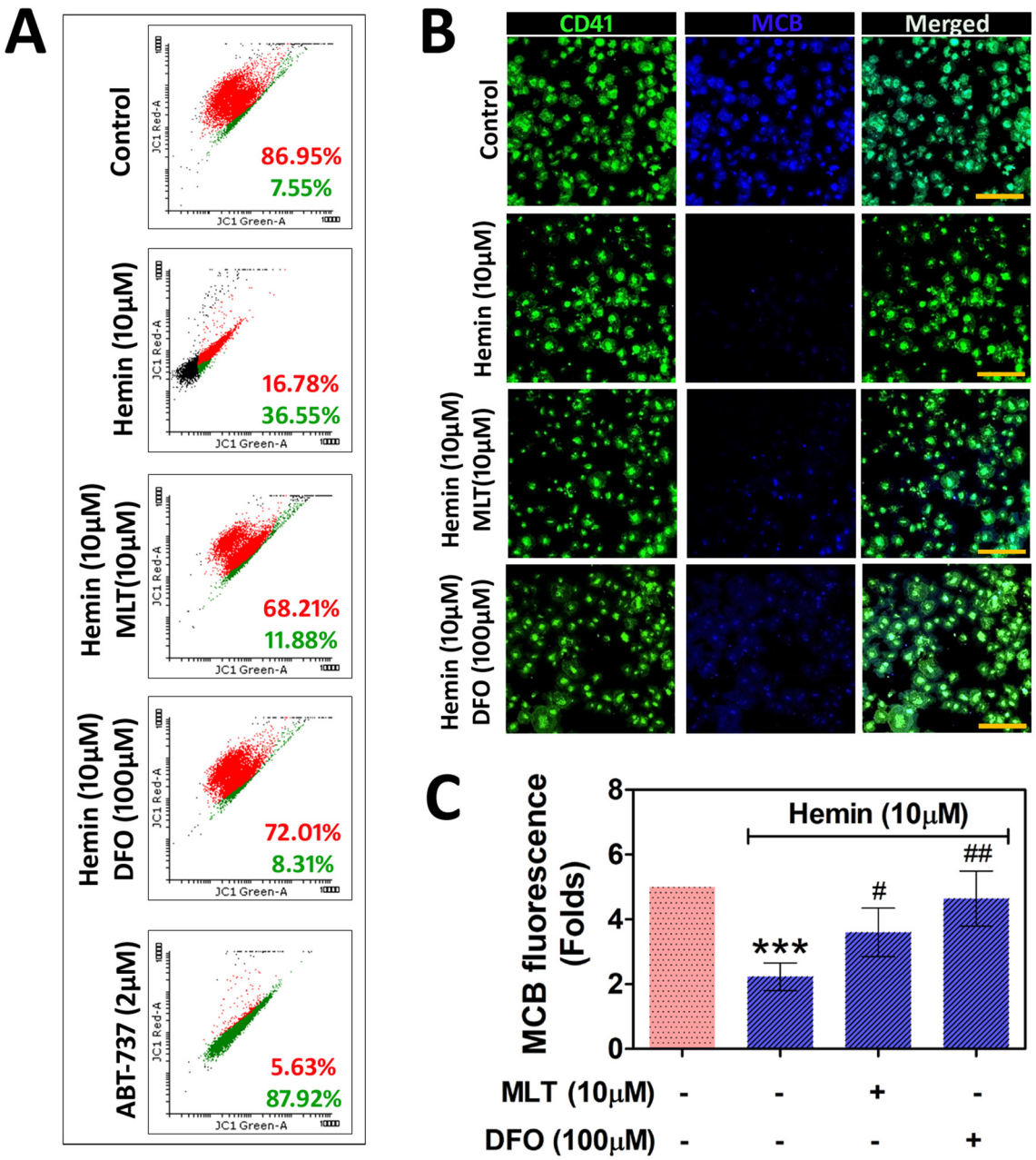

Fig. 4. Hemin-induced altered mitochondrial membrane potential (ΔΨm) and cellular glutathione (GSH) levels are restored by MLT: (A) FACS analysis of ΔΨm in hemin (10 μM) treated platelets in presence or absence of MLT (1 to 10 μM) and DFO (100 μM) using JC-1 dye. Evaluation of cellular GSH levels using monochlorobimane (MCB); which forms an adduct with cellular GSH. (B) Confocal microscopic and (C) FACS analysis of GSH level in hemin-treated platelets in the presence or absence of MLT (10 μM) and DFO (100 μM) using MCB dye. Platelets were marker with FITC-conjugated CD41 (platelet surface marker). The data is presented as mean ± SEM ($n = 5$) and analyzed using one-way ANOVA followed by Bonferroni posttests, $p^{*}/^{\#} < 0.05$, $p^{**}/^{\#\#} < 0.01$, $p^{***}/^{\#\#\#} < 0.001$; *significant compared to untreated platelets; #significant compared to hemin (10 μM) alone treated platelets.

2.17. Histopathology

Kidney and Lung tissue sections were examined for the hemin-induced destruction of kidney and lung tissues. Kidneys and Lungs were dissected from the hemin, hemin with MLT treated mice, fixed overnight in 10% neutral-buffered formalin and subjected to dehydration with different grades of alcohol and chloroform mixture. The processed tissues were then embedded in molten paraffin wax, and a 5 μm thickness sections were prepared using a microtome. The sections were then stained using hematoxylin and eosin (H&E) and observed under an Axio Imager. A2 microscope (Zeiss) and photographed [11].

2.18. Protein estimation

The protein estimation was done according to the method of Lowry et al. [35], using BSA as standard.

2.19. Statistical analysis

The data are presented as the mean ± SEM of at least four independent experiments. *In vitro* data was analyzed using one-way analysis of variance (ANOVA), followed by Tukey's *post hoc* test for multiple comparisons as applicable. *In vivo* data were analyzed using Student's *t*-test (unpaired), followed by Bonferroni *post hoc* analysis. All analyses were done using GraphPad Prism software (Version 5.0).

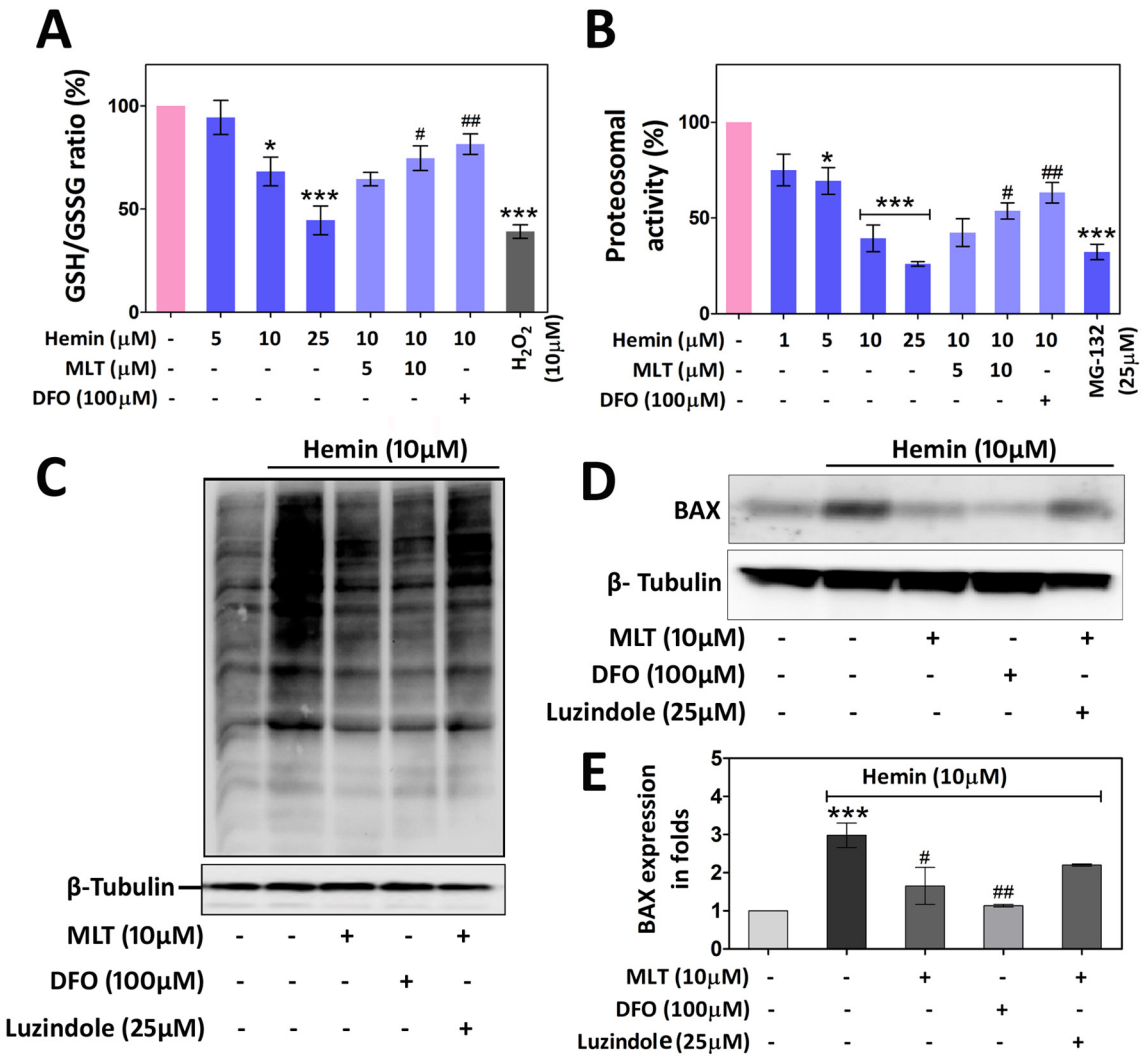

Fig. 5. Hemin-induced cellular depletion of GSH/GSSG content, decreased proteasomal activity, increased cytosolic ubiquitinated proteins, and BAX levels are ameliorated by MLT. Hemin (5–25 μM)-treated platelets in the presence or absence of MLT (1 to 10 μM), DFO (100 μM) and luzindole (25 μM) were assessed for (A) cellular GSH/GSSG using *o*-phthalaldehyde, (B) proteasomal activity using fluorogenic proteasome substrate (Suc-Leu-Leu-Val-Tyr-AMC), (C) ubiquitinated protein level by immunoblotting using (anti-ubiquitin Ab) and (D and E) cytosolic BAX level by immunoblotting with its densitometric analyses measured after normalization with cytosolic loading control, tubulin. MG-132 was taken as a standard proteasome inhibitor. The data is presented as mean ± SEM ($n = 5$) and analyzed using one-way ANOVA followed by Bonferroni posttests, $p^{*}/^{\#} < 0.05$, $p^{**}/^{\#\#} < 0.01$, $p^{***}/^{\#\#\#} < 0.001$; *significant compared to untreated platelets; $^{\#}$significant compared to hemin (10 μM) alone treated platelets.

3. Results

3.1. Hemin-induced platelet activation and ferroptosis-like death is mediated through ROS and is blocked by MLT

To determine whether hemin exerts a cytotoxic effect in platelets, cell viability and lactate dehydrogenase (LDH) release were evaluated in platelets treated with various doses of hemin. Hemin significantly reduced the cell viability (Fig. 1A) and increased LDH release in platelets (Fig. 1A) within 30 min of treatment, confirming the cytotoxic effect of hemin in platelets. To determine whether hemin induces platelet activation, surface P-selectin expression was examined. Interestingly, the FACS analysis showed that P-selectin level was significantly increased in the hemin-treated platelets in a dose dependent manner (Fig. 1B).

Previously we have demonstrated that hemin induces iron (Fe^{2+})-mediated platelet activation and ferroptosis-like death in platelets [4]. Therefore, in this study we evaluated the effect of MLT on hemin-induced toxicity. MLT (5 μM to 10 μM) significantly reduced platelet death (Fig. 1C) and LDH release in hemin-treated platelets (Fig. 1D). Deferoxamine (DFO); an intracellular iron chelator and ferrostatin-1 (FS-1); a well-known ferroptosis inhibitor, also significantly inhibited hemin-induced cell death and LDH release (Fig. 1C and D). In addition, FACS analysis confirmed that 10 μM MLT effectively inhibited the hemin-induced P-selectin expression in platelets compared to DFO (Fig. 1E and F).

This observation was further supported by fluorescence microscopy experiments, where we analyzed the actin dynamics in adherent platelets stained with Alexa Fluor-546 conjugated Phalloidin. Hemin at a dose of 10 μM induced filopodia-like structures in platelets, whereas at higher doses of hemin (25 μM) (Fig. 2A) these structures were destroyed, and presence of MLT and DFO significantly inhibited the hemin-induced filopodia formation (Fig. 2A). Further, as elevated ROS play a pivotal role in platelet activation, apoptosis, and thrombosis, we examined the effect of hemin on the generation of various endogenous ROS (H_2O_2, superoxide ($O_2\cdot^-$) and Hydroxyl radical ($\cdot$OH)) in platelets using DCFDA, Amplex RED, DHE and BODIPY C11 dyes. Hemin induced a dose-dependent increase in total ROS generation, H_2O_2 and Hydroxyl radical/lipid ROS generation in human platelets (Supplementary Fig. 1) but not superoxide radicals (Supplementary Fig. 1).

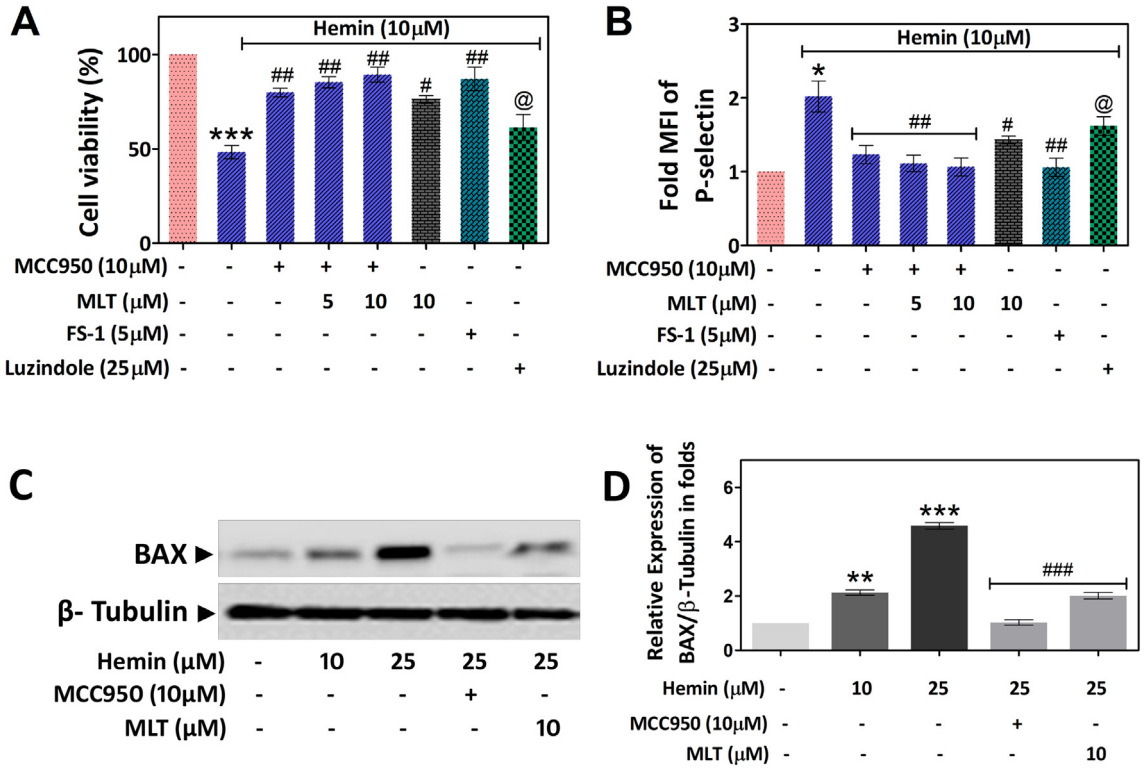

Fig. 6. Hemin-induced inflammasome activation leading to a decrease in platelet viability is mitigated by MLT. Hemin (10 μM)-treated platelets in the presence and absence of MLT (5 and 10 μM), MCC950 (20 μM), FS-1 (5 μM) and luzindole (25 μM) were evaluated for (A) cell viability using MTT assay, (B) FACS analysis of surface P-selectin expression using FITC conjugated P-selectin and (C and D) cytosolic BAX level using immunoblotting with its densitometric analyses measured after normalization with cytosolic loading control, β-tubulin. The data is presented as mean ± SEM ($n = 5$) and analyzed using one-way ANOVA followed by Bonferroni posttests, $p^{*}/^{\#} < 0.05$, $p^{**}/^{\#\#} < 0.01$, $p^{***}/^{\#\#\#} < 0.001$; *significant compared to untreated platelets; $^{\#}$significant compared to hemin (10 μM) alone treated platelets.

However, MLT and DFO treatment significantly restored the levels of ROS and lipid peroxide generation (Fig. 2B and C) (Supplementary Fig. 1). In order to investigate the source of ROS generation in hemin-treated platelets, diphenylene iodonium (DPI) an inhibitor of NADPH oxidase, that blocks the cytosolic ROS generation and Mito-TEMPO, a mitochondria targeted superoxide quencher was used. Both DPI and Mito-TEMPO failed to inhibit hemin-induced ROS generation suggesting that the principal source of ROS (·OH) generation is from labile iron in hemin-treated platelets (Supplementary Fig. 2). Further, hemin induced a significant mitochondrial cardiolipin oxidation in platelets, and presence of MLT (10 μM) and DFO (100 μM), completely restored the cardiolipin oxidative status (Fig. 2D and Supplementary Fig. 3).

Furthermore, the mitochondrial function was evaluated by assessing the mitochondrial membrane potential and levels of Bcl-2 family proteins (BAX, Bcl-2, Bcl-xL, BAK, BAD, Phospho-BAD, and BID) in hemin-treated platelets (Fig. 3A and B). FACS analysis and immunoblots indicated that hemin-induced a significant decrease in mitochondrial membrane potential, alteration in BAX, Bcl-2 and BAD proteins in the cytosolic fraction and an increase in the localization of BAX in the mitochondrial fraction (Fig. 3C). Meanwhile, there was a substantial decrease in anti-apoptotic Bcl-2 protein in mitochondrial fraction (Fig. 3C). However, treatment of MLT (10 μM) and DFO (100 μM) significantly restored the mitochondrial membrane potential (Fig. 4A and Supplementary Fig. 4) and cytosolic BAX level (Fig. 5D). The elevated ROS levels alter the endogenous antioxidant system like cellular glutathione (GSH). The confocal microscopy study and FACS analysis of hemin-treated platelets exhibited a significant decrease in the GSH level, and presence of MLT (10 μM) and DFO (100 μM) effectively restored the GSH level (Fig. 4B and C). As β-mercaptoethanol (β-ME) can enhance cysteine uptake through other pathways, platelets were treated with β-ME in the presence and absence of cysteine (250 μM) and MLT (10 μM) (Supplementary Fig. 5A and B). Interestingly, the treatment of platelets with β-ME and MLT significantly improved the cell viability and decreased ROS generation (Supplementary Fig. 5A and B) suggesting the involvement of system XC− in the hemin-mediated ferroptosis in platelets and the role of MLT in inhibiting it. Therefore, MLT not only inhibits hemin-induced platelet activation, it also blocks the ferroptotic cell death in platelets. Furthermore, hemin-induced a dose-dependent decrease in the GSH/GSSG ratio in the platelets and MLT significantly restored their levels (Fig. 5A). In support to this, we observed a significant change in the absorption spectra of hemin upon titration with various concentration of GSH and cysteine, suggesting that hemin forms an adduct with cellular GSH (Supplementary Fig. 6A and B).

3.2. Hemin-induced proteasomal inhibition and activation of inflammasome pathways are blocked by MLT

The proteasome is involved in the degradation of many short-term proteins that are required for cell survival. It has been demonstrated that the proteasome role in delimiting platelet lifespan through the constitutive elimination of the conformationally active BAX and inducing cell death in platelets. Since hemin dose-dependently elevated the level of pro-apoptotic Bcl-2 protein, BAX, we analyzed proteasomal peptidase activity in presence of different concentrations of Hemin (1–25 μM). Hemin (1–25 μM) attenuated proteasome function in a concentration-dependent (by 30% to 70%) fashion in platelets. Surprisingly, MLT (5–10 μM) and DFO (100 μM) significantly restored the proteasomal activity (Fig. 5B). Blocking of cellular proteasome activity exacerbates hemin-induced toxicity. As a result of accumulation of ubiquitin-tagged proteins, which provides the most direct evidence for impaired protein degradation capacity in hemin-treated platelets. In

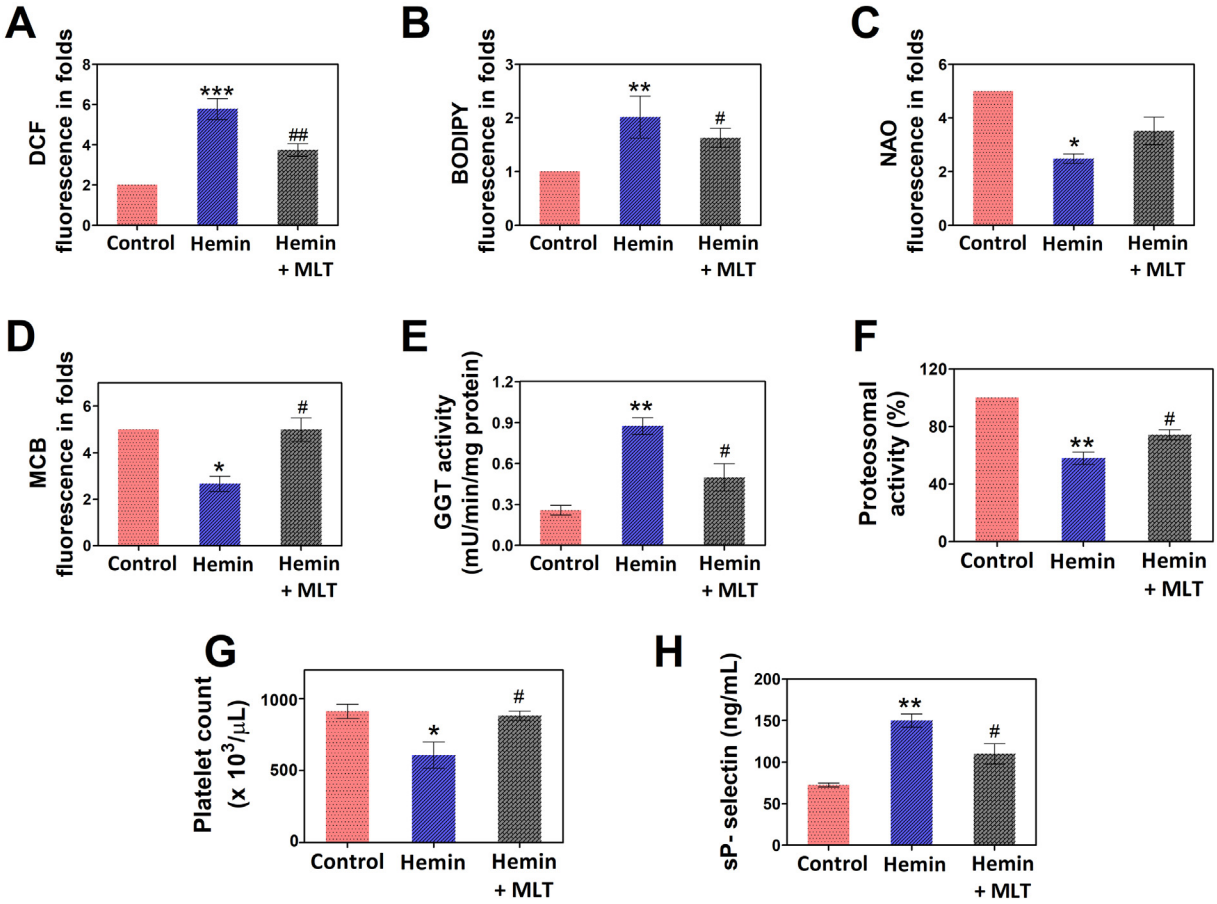

Fig. 7. Hemin-induced toxicity on circulatory platelets *in vivo* is prevented by MLT: Male Swiss albino mice (8- to 10-week-old) weighing 20–25 g was injected with hemin (50 μmol/kg body weight) (i.p.) for 72 h, followed by MLT (20 mg/kg body weight) (i.p.) injection after 2 h of hemin treatment. Fluorometric analysis of platelets isolated from experimental animals stained with (A) DCFDA for ROS generation, (B) BODIPY for lipid peroxide generation and lipid peroxidation, (C) NAO for cardiolipin oxidation and (D) MCB for cellular glutathione level. Platelets isolated from experimental animals were assessed for (E) GGT activity and (F) proteasomal activity. (G) Automated analysis of platelet count in blood drawn from experimental animals. (H) ELISA based quantification of soluble P-selectin (sP-selectin) level in plasma obtained from treated mice blood. The data is presented as mean ± SEM ($n = 5$) and analyzed using one-way ANOVA followed by Student's *t*-test (unpaired), $p^{*}/^{\#} < 0.05$, $p^{**}/^{\#\#} < 0.01$, $p^{***}/^{\#\#\#} < 0.001$; *significant compared to control group; #significant compared to hemin-treated group.

order to demonstrate the effect of hemin on the levels of ubiquitinated proteins and BAX, we evaluated hemin-treated platelets in presences or absences of MLT, DFO, and Luzindole; a selective MLT receptor (MT2) antagonist, using immunoblots. Hemin (10 μM) significantly increased the levels of ubiquitinated proteins and BAX protein, and both MLT and DFO significantly restored it (Fig. 5C). In addition, MLT pre-treated with luzindole showed significant attenuation of hemin-induced protein ubiquitination and BAX level, indicating that MLT protects platelets from hemin-induced toxicity through MT2 receptor-mediated events (Fig. 5D and E).

Further, to gain insight into the molecular signalling pathway through which hemin induces platelet activation and ferroptosis-like death in platelets, we evaluated the downstream signalling of hemin and effect of MLT on it. Hemin significantly induced activation of NLRP-3 in platelets. At first, we evaluated platelet proteasomal activity in presence of Tin-protoporphyrin IX (SnPP), a heme oxygenase-1 (HO-1) specific inhibitor. In presence of SnPP there was an increased proteasomal inhibition when compared to hemin alone suggesting that iron-containing porphyrin is essential to inhibit proteasomes (Supplementary Fig. 7). Interestingly, MLT (10 μM) significantly restored the proteasome activity, and we further confirmed using luzindole (Supplementary Fig. 7). Further, we evaluated the effect of MCC950; a selective inhibitor of NLRP3 on hemin-induced platelet activation and death. Interestingly, MCC950 significantly improved cell viability (Fig. 6A), decreased surface P-selectin expression (Fig. 6B) and BAX levels (Fig. 6C and D) in hemin-treated platelets. MLT treatment enhanced the protective efficacy and MLT-treated along with MCC950 and in presence of luzindole the effect of MLT was reduced indicating involvement of MT2. The above observations clearly indicated that hemin induces inflammasome formation, which further contributes to platelet activation or death and MLT effectively protected platelets from inflammasome-induced platelet activation and death.

3.3. Hemin-induced oxidative damage and toxicity are mitigated by MLT in vivo

To correlate our *in vitro* findings in an animal model, the effect of MLT on hemin-induced platelet activation and death was studied in Swiss albino mice. In order to determine the effective dose and time of MLT, which can ameliorate the hemin-induced toxicity, mice were injected with hemin (50 μmol/kg body weight) and a group of mice received MLT (20 mg/kg body weight) (i.p.), after 4 h of hemin injection. Hemin-induced toxicity on platelets and systemic organs were assessed after 24 h of hemin injection. The one-time injection of hemin (50 μmol/kg body weight) did not induce toxicity up to 24 h [Data not shown]. Therefore, mice were administrated a daily dose of hemin (50 μmol/kg body weight) for 3 days (72 h) and a group of mice received MLT (20 mg/kg body weight) (i.p.), after 2 h of hemin injection. This induced a significant hemin toxicity and protective efficacy of MLT. Therefore, 72 h of hemin-treatment was considered for our

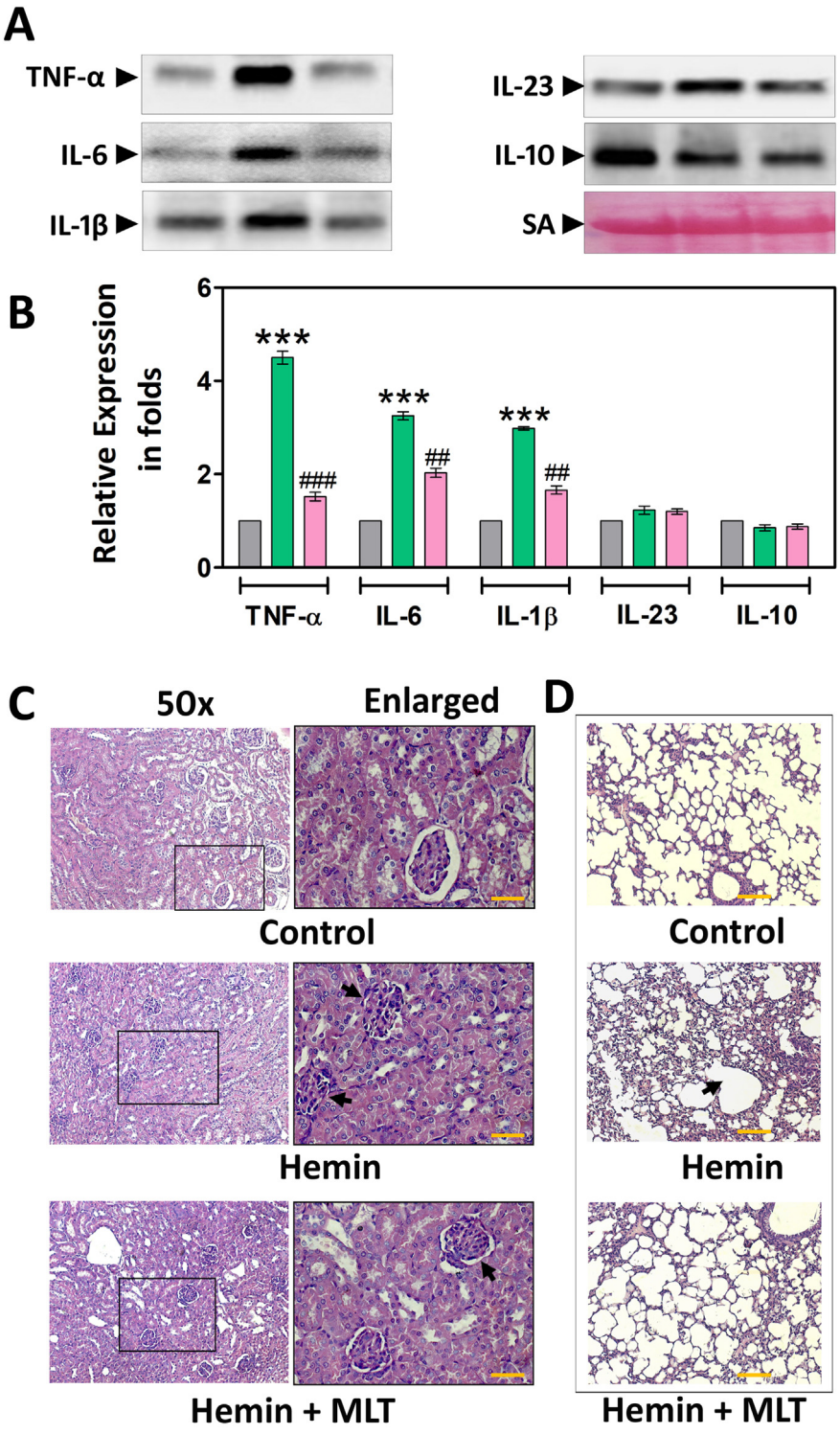

Fig. 8. Hemin-induced modulation of serum cytokines levels, and kidney and lung tissue destruction *in vivo* are mitigated by MLT: (A) Various cytokines (TNF-α, IL-1β, IL-6, IL-23, and IL-10) level were assessed in serum obtained from the treated mice groups using immunoblotting along with (B) its densitometry analysis and the image of the corresponding Ponceau-stained PVDF membrane was served as loading control. The membrane was cut based on the molecular weight, probed with the antibody of interest. Histological analysis of (C) kidney and (D) lung tissue section obtained from the treated mice groups using Hematoxylin-Eosin (H&E) staining. The data are presented as mean ± SEM ($n = 5$) and analyzed using one-way ANOVA followed by Student's *t*-test (unpaired). $p^{*}/^{\#} < 0.05$, $p^{**}/^{\#\#} < 0.01$, $p^{***}/^{\#\#\#} < 0.001$; *significant compared to control group; $^{\#}$significant compared to hemin-treated group.

experiments. Further, we evaluated the levels of ROS, lipid peroxidation, cardiolipin oxidation, cellular GSH level in hemin and MLT-treated mice platelets. MLT-treated mice showed significantly decreased level of ROS generation, lipid peroxidation, cardiolipin oxidation and increased level of GSH as compared to the hemin-treated group (Fig. 7A–D). In addition, we evaluated the GGT activity and proteasomal activity in hemin-treated mice platelets. Hemin treatment significantly decreased the GGT (Fig. 7E) and proteasomal activity (Fig. 7F), however, MLT administration restored the above-mentioned activities significantly. As intravascular hemolysis leads to low platelet count (thrombocytopenia) and platelet activation [36], we investigated the effect of hemin treatment on the circulating platelet count. Hemin (50 μmol/kg body weight) treatment resulted in a decreased number of circulating platelets in mice. Interestingly, MLT administration significantly rescued the circulatory platelets (Fig. 7G). Besides, P-selectin from activated platelets contributes directly to vascular inflammation and thrombosis in many vascular diseases [37]. Therefore, we determined the plasma soluble P-selectin (sP-selectin) levels in hemin-treated mice. Hemin-induced a significant increase in sP-selectin and MLT administration significantly reduced the levels of plasma sP-

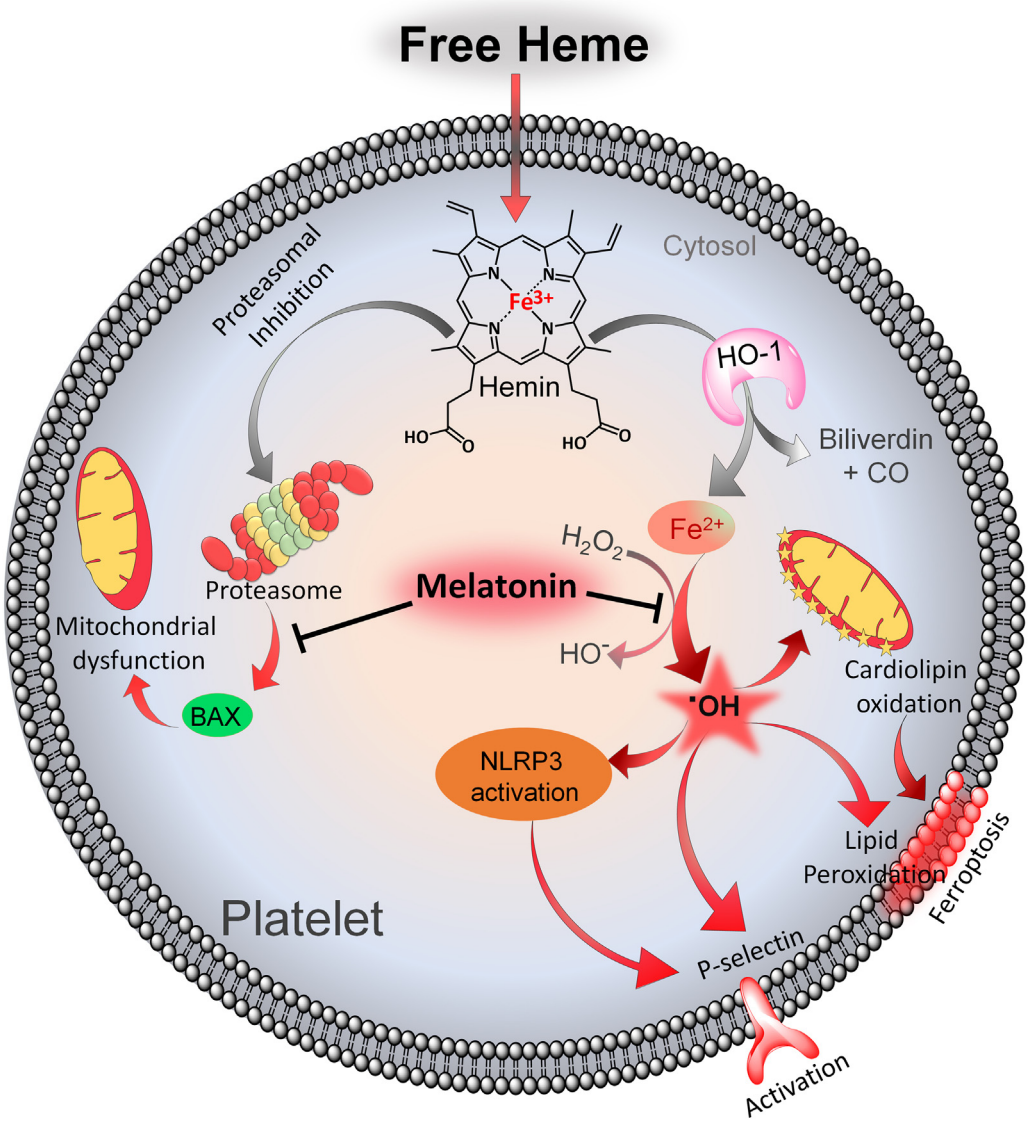

Fig. 9. Proposed mechanism of action of MLT in protecting platelets from hemin-induced toxicity.

selectin as compared to the hemin-treated mice (Fig. 7H).

Further, serum levels of pro-inflammatory mediators including IL-1β, TNF-α, IL-6, and IL-23 were significantly increased in the hemin-injected group, whereas anti-inflammatory cytokine IL-10 was significantly reduced compared to the saline control group and upon MLT administration there was significant restoration of these pro-inflammatory and anti-inflammatory cytokines (Fig. 8A and B). The kidney and lung damage were further substantiated by histopathology studies using H&E staining. The critical examination of photomicrographs of the control kidney tissue section depicted the normal architecture. The hemin-injected mice kidney tissue section showed glomerular congestion and destructed epithelial cells (Fig. 8C). On the other hand, destruction of the alveolar architecture with distension of the alveolar sacs and infiltration of inflammatory cells was observed in lung tissue section of hemin-injected mice (Fig. 8D). Interestingly, MLT administration significantly inhibited kidney and lung tissue destruction.

4. Discussion

Several studies including ours have demonstrated that the platelets being anuclear undergo mitochondria-mediated apoptosis. Several chemical and natural molecules can induce premature apoptosis in platelets [12]. Previously, we have shown that hemoglobin and its derivatives like methemoglobin and bilirubin are capable to drive platelet activation and mitochondria-mediated apoptosis with classical caspase activation [11,31]. However, platelets apart from classical mitochondria-mediated apoptosis can undergo ROS-lipid peroxidation driven ferroptosis [3–5]. Ferroptosis, a unique and non-classical type of cell death, independent of caspase activation and is mediated through accumulation of lipid ROS, and depletion of cellular GSH [4,38,39]. We have shown that hemin induces platelet activation and ferroptosis mediated through lipid peroxidation and ROS release. As MLT is a potent lipid ROS quencher and cytoprotective molecule, in this study we determined the ability of MLT to inhibit Hemin-induced ferroptosis in platelets. The cytoprotective abilities of MLT are highly appreciated. Besides regulating the circadian rhythms of biological clock in mammals, MLT is deemed as one of the potent endogenous antioxidants demonstrating protective abilities against cardiovascular, diabetes, cytotoxicity and neurological complications [40,41]. MLT is reported to protect amitriptyline-induced hepatotoxicity by quenching ROS and lipid peroxidation [42]. In Bone marrow mesenchymal stem cells (MSCs), MLT significantly enhanced survivability of hypoxia and serum deprived MSCs by inhibiting MAPK signalling [43]. Previously, we have

demonstrated that the anti-venom and anti-apoptotic abilities of MLT, which largely due to their radical trapping property [17,21,22].

Hemin, a catabolic product of hemoglobin, can be high in circulation due to increased intravascular hemolysis/hemorrhagic strokes or during hemolysis associated disorders [30,36,44–46]. However, hemin is also used as a pharmacological agent to treat porphyria or acute intermittent porphyria [47]. Herein, we demonstrate that hemin induces platelet activation and ferroptosis in platelets both *in vitro* and *in vivo*, and MLT significantly neutralizes hemin induced toxicity and rescue platelets. Hemin caused platelet death through increased ROS, lipid peroxidation and GSH/GSSG depletion by disrupting endogenous glutathione cycle. The substantial depletion in the GSH level indicates that the hemin-mediated ferroptosis may occur through inhibition of system Xc– that transports extracellular cystine into the cell for the biosynthesis of GSH [48]. In addition, hemin activated the platelets both *in vitro* and *in vivo* by inducing p-selectin expression. Further evaluation of the mitochondrial health revealed that hemin significantly alters mitochondrial membrane potential contributing to the altered Bcl-2 family of proteins (BAX, Bcl-2, Bcl-xL, BAK, BAD, Phospho-BAD, and BID) that regulate cell death. However, previously we have shown mitochondria-independent cell death [11,12,31]. In addition, DFO and FS-1 effectively inhibited hemin-induced platelet activation and death by interfering in above discussed key events suggesting hemin drives iron-dependent activation and death of platelets, which is ferroptosis [4]. Interestingly, MLT remarkably outplayed hemin-induced platelet activation and ferroptosis acting through MT2 receptor to restore mitochondrial health and glutathione homeostasis by inhibiting hemin-induced ROS and lipid peroxidation. MT2 receptor is a major G protein-coupled receptor, which primarily facilitates the melatonin signalling [49].

Both hemoglobin and hemin are cytotoxic and genotoxic in human colon cells *via* free radical mechanisms [50]. Hemin is also shown to be cytotoxic to colonic epithelial cells by targeting translocator protein [51]. Although there are limited evidences that hemin alters Bcl-2 family proteins, we have previously demonstrated that the unconjugated bilirubin induces platelet apoptosis targeting mitochondria and Bcl-2 family proteins [11,31]. All these studies emphasize the cytotoxic nature of hemin, which are in line with our results.

Further comprehensive evaluation into the hemin-induced platelet activation and ferroptosis in platelets exposed that proteasome activity and inflammasome activation are two key events. Proteasome enhances ubiquitination of target proteins and mediates the degradation of short-lived ubiquitinated proteins, which are necessary for cell survival. It reduces platelet survivability in circulation by aborting conformationally active BAX protein and by inducing apoptosis-related changes in platelets [52,53]. Both Bcl-2 family of proteins and proteasome system are considered to be as an essential internal timer regulating platelet lifespan, a dysregulation in this process stimulates untimely apoptosis [52,53]. We demonstrate that hemin significantly modulated Bcl-2 family proteins and inhibited proteasome activity in platelets thus causing uncontrolled premature platelet death both *in vitro* and *in vivo*. However, MLT effectively counteracts hemin-induced proteasome inhibition and controls the expression of Bcl-2 family proteins, thus preventing cell death both *in vitro* and *in vivo*.

Furthermore, we show that hemin significantly activates inflammasome (NLRP-3) mediated through hydroxyl radical. Inflammasome activation in nucleated cells is well characterized, nevertheless platelets constitutively express the inflammasome components NLRP3 and ASC suggesting existence of assembled inflammasomes in platelets [54]. Platelet activation agonists can stimulate inflammasome activation in platelets. Both increased levels of ROS and cytokines like IL-1β contribute to the inflammasome activation in platelets [55]. Platelet NLRP3 inflammasome is reported to mediate platelet activation and aggregation *via* increased expression of Caspase-1 and increased secretion of IL-1β [56,57]. We show that hemin induces NLRP3 inflammasome to stimulate platelet activation *in vitro*. In addition, elevated serum levels of several key inflammatory cytokines including IL-1β, TNF-α, IL-23 and IL-6 *in vivo* along with sP-selectin indicates that hemin induces inflammasome activation along with key pro-inflammatory cytokines. Interestingly, MLT effectively inhibited hemin-induced platelet activation mediated through NLRP3 inflammasome.

In summary, the current findings demonstrate for the first time the unexplored pathway underlying thrombotic complications under severe hemolysis (Fig. 9). Although, the involvement of hemin in thrombosis has been studied in hemolytic conditions, here we report that hemin-induces ferroptosis in platelets *via* increased ROS/lipid peroxidation/glutathione depletion, whereas the platelet activation is mediated *via* proteasome and inflammasome activation. More importantly, MLT significantly abolished hemin-induced both platelet activation and ferroptosis. Therefore, our study demonstrates that MLT can be considered as a novel treatment strategy in hemolytic disorders.

Author contributions

KSG, KK and SKN designed the study; SKN performed all the experiments; KSG, SKN and HM analyzed the data; SKN and HM wrote the manuscript; KSG conceived and directly supervised the study and extensively edited the manuscript. All authors reviewed and edited the manuscript.

Transparency document

The Transparency document associated with this article can be found, in online version.

Acknowledgment

Authors thank Prof. G. Mugesh, Inorganic and Physical Chemistry, Indian Institute of Science-Bangalore, for his kind support and encouragement during the study. Authors thank Central Instrumentation Facility, Indian Institute of Science-Bangalore, and Institute of excellence, University of Mysore. Authors also thank Ms. Vishalakshi GJ, Dr. Jagadhish and Mr. Manikanta University of Mysore, Mysuru, for their kind help during the study. KSG acknowledges the funding from the DST-SERB (EEQ/2016/000280). KK acknowledges the funding from the DST-SERB (EEQ/2016/000193) and UGC-SAP (F3-14/2012 SAP-II).

Declaration of Competing Interest

The authors declare that they have no conflicts of interest with the contents of this article.

Appendix A. Supplementary data

Supplementary data to this article can be found online at https://doi.org/10.1016/j.bbadis.2019.05.009.

References

[1] J.P. Silva, O.P. Coutinho, Free radicals in the regulation of damage and cell death - basic mechanisms and prevention, Drug Discov Ther. 4 (2010) 144–167.
[2] M. Guha, P. Maity, V. Choubey, K. Mitra, R.J. Reiter, U. Bandyopadhyay, Melatonin inhibits free radical-mediated mitochondrial-dependent hepatocyte apoptosis and liver damage induced during malarial infection, J. Pineal Res. 43 (2007) 372–381, https://doi.org/10.1111/j.1600-079X.2007.00488.x.
[3] B.R. Stockwell, J.P. Friedmann Angeli, H. Bayir, A.I. Bush, M. Conrad, S.J. Dixon, S. Fulda, S. Gascón, S.K. Hatzios, V.E. Kagan, K. Noel, X. Jiang, A. Linkermann, M.E. Murphy, M. Overholtzer, A. Oyagi, G.C. Pagnussat, J. Park, Q. Ran, C.S. Rosenfeld, K. Salnikow, D. Tang, F.M. Torti, S.V. Torti, S. Toyokuni, K.A. Woerpel, D.D. Zhang, Ferroptosis: a regulated cell death nexus linking metabolism, redox biology, and disease, Cell. 171 (2017) 273–285, https://doi.org/10.1016/j.cell.2017.09.021.
[4] S.K. NaveenKumar, B.N. SharathBabu, M. Hemshekhar, K. Kemparaju, K.S. Girish, G. Mugesh, The role of reactive oxygen species and ferroptosis in heme-mediated

activation of human platelets, ACS Chem. Biol. 13 (2018) 1996–2002, https://doi.org/10.1021/acschembio.8b00458.
[5] W.S. Yang, K.J. Kim, M.M. Gaschler, M. Patel, M.S. Shchepinov, B.R. Stockwell, Peroxidation of polyunsaturated fatty acids by lipoxygenases drives ferroptosis, Proc. Natl. Acad. Sci. U. S. A. 113 (2016) E4966–E4975, https://doi.org/10.1073/pnas.1603244113.
[6] W.S. Yang, B.R. Stockwell, Ferroptosis: death by lipid peroxidation, Trends Cell Biol. 26 (2016) 165–176, https://doi.org/10.1016/j.tcb.2015.10.014.
[7] S.J. Dixon, K.M. Lemberg, M.R. Lamprecht, R. Skouta, E.M. Zaitsev, C.E. Gleason, D.N. Patel, A.J. Bauer, A.M. Cantley, W.S. Yang, B. Morrison, B.R. Stockwell, Ferroptosis: an iron-dependent form of non-apoptotic cell death, Cell 149 (2012) 1060–1072, https://doi.org/10.1016/j.cell.2012.03.042.
[8] T. Sehm, Z. Fan, A. Ghoochani, M. Rauh, T. Engelhorn, G. Minakaki, A. Dörfler, J. Klucken, M. Buchfelder, I.Y. Eyüpoglu, N. Savaskan, Sulfasalazine impacts on ferroptotic cell death and alleviates the tumor microenvironment and glioma-induced brain edema, Oncotarget. 7 (2016) 36021–36033, https://doi.org/10.18632/oncotarget.8651.
[9] C. Wu, W. Zhao, J. Yu, S. Li, L. Lin, X. Chen, Induction of ferroptosis and mitochondrial dysfunction by oxidative stress in PC12 cells, Sci. Rep. 8 (2018) 574, , https://doi.org/10.1038/s41598-017-18935-1.
[10] Z. Qiu, S. Lei, B. Zhao, Y. Wu, W. Su, M. Liu, Q. Meng, B. Zhou, Y. Leng, Z.-Y. Xia, NLRP3 inflammasome activation-mediated pyroptosis aggravates myocardial ischemia/reperfusion injury in diabetic rats, Oxidative Med. Cell. Longev. 2017 (2017) 9743280, , https://doi.org/10.1155/2017/9743280.
[11] S.K. NaveenKumar, R.M. Thushara, M.S. Sundaram, M. Hemshekhar, M. Paul, C. Thirunavukkarasu, null Basappa, G. Nagaraju, S.C. Raghavan, K.S. Girish, K. Kemparaju, K.S. Rangappa, Unconjugated bilirubin exerts pro-apoptotic effect on platelets via p38-MAPK activation, Sci. Rep. 5 (2015) 15045, , https://doi.org/10.1038/srep15045.
[12] R.M. Thushara, M. Hemshekhar, null Basappa, K. Kemparaju, K.S. Rangappa, K.S. Girish, Biologicals, platelet apoptosis and human diseases: an outlook, Crit. Rev. Oncol. Hematol. 93 (2015) 149–158, https://doi.org/10.1016/j.critrevonc.2014.11.002.
[13] O. Zilka, R. Shah, B. Li, J.P. Friedmann Angeli, M. Griesser, M. Conrad, D.A. Pratt, On the mechanism of cytoprotection by ferrostatin-1 and liproxstatin-1 and the role of lipid peroxidation in ferroptotic cell death, ACS Cent Sci. 3 (2017) 232–243, https://doi.org/10.1021/acscentsci.7b00028.
[14] C. Cajochen, K. Kräuchi, A. Wirz-Justice, Role of melatonin in the regulation of human circadian rhythms and sleep, J. Neuroendocrinol. 15 (2003) 432–437.
[15] C.J. Morris, D. Aeschbach, F.A.J.L. Scheer, Circadian system, sleep and endocrinology, Mol. Cell. Endocrinol. 349 (2012) 91–104, https://doi.org/10.1016/j.mce.2011.09.003.
[16] R.J. Reiter, D.-X. Tan, J.C. Mayo, R.M. Sainz, J. Leon, Z. Czarnocki, Melatonin as an antioxidant: biochemical mechanisms and pathophysiological implications in humans, Acta Biochim. Pol. 50 (2003) 1129–1146 (doi:0350041129).
[17] R.D. Sharma, G.D. Katkar, M.S. Sundaram, M. Paul, S.K. NaveenKumar, B. Swethakumar, M. Hemshekhar, K.S. Girish, K. Kemparaju, Oxidative stress-induced methemoglobinemia is the silent killer during snakebite: a novel and strategic neutralization by melatonin, J. Pineal Res. 59 (2015) 240–254, https://doi.org/10.1111/jpi.12256.
[18] P. Medrano-Campillo, H. Sarmiento-Soto, N. Álvarez-Sánchez, A.I. Álvarez-Ríos, J.M. Guerrero, I. Rodríguez-Prieto, M.J. Castillo-Palma, P.J. Lardone, A. Carrillo-Vico, Evaluation of the immunomodulatory effect of melatonin on the T-cell response in peripheral blood from systemic lupus erythematosus patients, J. Pineal Res. 58 (2015) 219–226, https://doi.org/10.1111/jpi.12208.
[19] A. Galano, D.X. Tan, R.J. Reiter, On the free radical scavenging activities of melatonin's metabolites, AFMK and AMK, J. Pineal Res. 54 (2013) 245–257, https://doi.org/10.1111/jpi.12010.
[20] R. Hardeland, Melatonin and inflammation-story of a double-edged blade, J. Pineal Res. 65 (2018) e12525, , https://doi.org/10.1111/jpi.12525.
[21] Z.-W. Zou, T. Liu, Y. Li, P. Chen, X. Peng, C. Ma, W.-J. Zhang, P.-D. Li, Melatonin suppresses thyroid cancer growth and overcomes radioresistance via inhibition of p65 phosphorylation and induction of ROS, Redox Biol. 16 (2018) 226–236, https://doi.org/10.1016/j.redox.2018.02.025.
[22] G.D. Katkar, M.S. Sundaram, M. Hemshekhar, D.R. Sharma, M.S. Santhosh, K. Sunitha, K.S. Rangappa, K.S. Girish, K. Kemparaju, Melatonin alleviates Echis carinatus venom-induced toxicities by modulating inflammatory mediators and oxidative stress, J. Pineal Res. 56 (2014) 295–312, https://doi.org/10.1111/jpi.12123.
[23] C. Rodriguez, J.C. Mayo, R.M. Sainz, I. Antolín, F. Herrera, V. Martín, R.J. Reiter, Regulation of antioxidant enzymes: a significant role for melatonin, J. Pineal Res. 36 (2004) 1–9.
[24] R.J. Reiter, J.C. Mayo, D.-X. Tan, R.M. Sainz, M. Alatorre-Jimenez, L. Qin, Melatonin as an antioxidant: under promises but over delivers, J. Pineal Res. 61 (2016) 253–278, https://doi.org/10.1111/jpi.12360.
[25] F. Camacho-Alonso, I. Urrutia-Rodríguez, D. Oñate-Cabrerizo, R.E. Oñate-Sánchez, F.J. Rodríguez-Lozano, Cytoprotective effects of melatonin on zoledronic acid-treated human osteoblasts, J. Craniomaxillofac. Surg. 45 (2017) 1251–1257, https://doi.org/10.1016/j.jcms.2017.04.006.
[26] T. Fan, H. Pi, M. Li, Z. Ren, Z. He, F. Zhu, L. Tian, M. Tu, J. Xie, M. Liu, Y. Li, M. Tan, G. Li, W. Qing, R.J. Reiter, Z. Yu, H. Wu, Z. Zhou, Inhibiting MT2-TFE3-dependent autophagy enhances melatonin-induced apoptosis in tongue squamous cell carcinoma, J. Pineal Res. 64 (2018), https://doi.org/10.1111/jpi.12457.
[27] H. Pan, H. Wang, Y. Jia, Q. Wang, L. Li, Q. Wu, L. Chen, VPA and MEL induce apoptosis by inhibiting the Nrf2-ARE signaling pathway in TMZ-resistant U251 cells, Mol. Med. Rep. 16 (2017) 908–914, https://doi.org/10.3892/mmr.2017.6621.
[28] K.S. Girish, M. Paul, R.M. Thushara, M. Hemshekhar, M. Shanmuga Sundaram, K.S. Rangappa, K. Kemparaju, Melatonin elevates apoptosis in human platelets via ROS mediated mitochondrial damage, Biochem. Biophys. Res. Commun. 438 (2013) 198–204, https://doi.org/10.1016/j.bbrc.2013.07.053.
[29] G. Chen, D. Zhang, T.A. Fuchs, D. Manwani, D.D. Wagner, P.S. Frenette, Heme-induced neutrophil extracellular traps contribute to the pathogenesis of sickle cell disease, Blood. 123 (2014) 3818–3827, https://doi.org/10.1182/blood-2013-10-529982.
[30] E.M. Sparkenbaugh, P. Chantrathammachart, S. Wang, W. Jonas, D. Kirchhofer, D. Gailani, A. Gruber, R. Kasthuri, N.S. Key, N. Mackman, R. Pawlinski, Excess of heme induces tissue factor-dependent activation of coagulation in mice, Haematologica. 100 (2015) 308–314, https://doi.org/10.3324/haematol.2014.114728.
[31] S.K. NaveenKumar, M. Hemshekhar, M.S. Sundaram, K. Kemparaju, K.S. Girish, Cell-free methemoglobin drives platelets to apoptosis via mitochondrial ROS-mediated activation of JNK and p38 MAP kinase, Biochem. Biophys. Res. Commun. 491 (2017) 183–191, https://doi.org/10.1016/j.bbrc.2017.07.073.
[32] S.M. Schoenwaelder, K.E. Jarman, E.E. Gardiner, M. Hua, J. Qiao, M.J. White, E.C. Josefsson, I. Alwis, A. Ono, A. Willcox, R.K. Andrews, K.D. Mason, H.H. Salem, D.C.S. Huang, B.T. Kile, A.W. Roberts, S.P. Jackson, Bcl-xL-inhibitory BH3 mimetics can induce a transient thrombocytopathy that undermines the hemostatic function of platelets, Blood 118 (2011) 1663–1674, https://doi.org/10.1182/blood-2011-04-347849.
[33] S. Kumari, S.N. Chaurasia, M.K. Nayak, R.L. Mallick, D. Dash, Sirtuin inhibition induces apoptosis-like changes in platelets and thrombocytopenia, J. Biol. Chem. 290 (2015) 12290–12299, https://doi.org/10.1074/jbc.M114.615948.
[34] M.K. Nayak, A. Dash, N. Singh, D. Dash, Aspirin delimits platelet life span by proteasomal inhibition, PLoS One 9 (2014) e105049, , https://doi.org/10.1371/journal.pone.0105049.
[35] O.H. Lowry, N.J. Rosebrough, A.L. Farr, R.J. Randall, Protein measurement with the Folin phenol reagent, J. Biol. Chem. 193 (1951) 265–275.
[36] R. Singhal, G.K. Annarapu, A. Pandey, S. Chawla, A. Ojha, A. Gupta, M.A. Cruz, T. Seth, P. Guchhait, Hemoglobin interaction with GP1bα induces platelet activation and apoptosis: a novel mechanism associated with intravascular hemolysis, Haematologica. 100 (2015) 1526–1533, https://doi.org/10.3324/haematol.2015.132183.
[37] H.M. Amin, S. Ahmad, J.M. Walenga, D.A. Hoppensteadt, H. Leitz, J. Fareed, Soluble P-selectin in human plasma: effect of anticoagulant matrix and its levels in patients with cardiovascular disorders, Clin. Appl. Thromb. Hemost. 6 (2000) 71–76.
[38] M. Conrad, V.E. Kagan, H. Bayir, G.C. Pagnussat, B. Head, M.G. Traber, B.R. Stockwell, Regulation of lipid peroxidation and ferroptosis in diverse species, Genes Dev. 32 (2018) 602–619, https://doi.org/10.1101/gad.314674.118.
[39] Y. Xie, W. Hou, X. Song, Y. Yu, J. Huang, X. Sun, R. Kang, D. Tang, Ferroptosis: process and function, Cell Death Differ. 23 (2016) 369–379, https://doi.org/10.1038/cdd.2015.158.
[40] L. Yu, C. Fan, Z. Li, J. Zhang, X. Xue, Y. Xu, G. Zhao, Y. Yang, H. Wang, Melatonin rescues cardiac thioredoxin system during ischemia-reperfusion injury in acute hyperglycemic state by restoring Notch1/Hes1/Akt signaling in a membrane receptor-dependent manner, J. Pineal Res. 62 (2017), https://doi.org/10.1111/jpi.12375.
[41] G. Favero, L. Franceschetti, F. Bonomini, L.F. Rodella, R. Rezzani, Melatonin as an anti-inflammatory agent modulating inflammasome activation, Int. J. Endocrinol. 2017 (2017) 1835195, , https://doi.org/10.1155/2017/1835195.
[42] S. Taziki, M.R. Sattari, S. Dastmalchi, M.A. Eghbal, Cytoprotective effects of melatonin against amitriptyline-induced toxicity in isolated rat hepatocytes, Adv. Pharm. Bull. 5 (2015) 329–334, https://doi.org/10.15171/apb.2015.046.
[43] F. Wang, H. Zhou, Z. Du, X. Chen, F. Zhu, Z. Wang, Y. Zhang, L. Lin, M. Qian, X. Zhang, X. Li, A. Hao, Cytoprotective effect of melatonin against hypoxia/serum deprivation-induced cell death of bone marrow mesenchymal stem cells in vitro, Eur. J. Pharmacol. 748 (2015) 157–165, https://doi.org/10.1016/j.ejphar.2014.09.033.
[44] N. Conran, C.B. Almeida, Hemolytic vascular inflammation: an update, Rev. Bras. Hematol. Hemoter. 38 (2016) 55–57, https://doi.org/10.1016/j.bjhh.2015.10.004.
[45] D.J. Schaer, P.W. Buehler, A.I. Alayash, J.D. Belcher, G.M. Vercellotti, Hemolysis and free hemoglobin revisited: exploring hemoglobin and hemin scavengers as a novel class of therapeutic proteins, Blood 121 (2013) 1276–1284, https://doi.org/10.1182/blood-2012-11-451229.
[46] M.T. Gladwin, Cardiovascular complications and risk of death in sickle-cell disease, Lancet. 387 (2016) 2565–2574, https://doi.org/10.1016/S0140-6736(16)00647-4.
[47] M. Balwani, R.J. Desnick, The porphyrias: advances in diagnosis and treatment, Blood. 120 (2012) 4496–4504, https://doi.org/10.1182/blood-2012-05-423186.
[48] M. Sato, R. Kusumi, S. Hamashima, S. Kobayashi, S. Sasaki, Y. Komiyama, T. Izumikawa, M. Conrad, S. Bannai, H. Sato, The ferroptosis inducer erastin irreversibly inhibits system x c − and synergizes with cisplatin to increase cisplatin's cytotoxicity in cancer cells, Sci. Rep. 8 (2018) 968, , https://doi.org/10.1038/s41598-018-19213-4.
[49] D. Liu, N. Wei, H.-Y. Man, Y. Lu, L.-Q. Zhu, J.-Z. Wang, The MT2 receptor stimulates axonogenesis and enhances synaptic transmission by activating Akt signaling, Cell Death Differ. 22 (2015) 583–596, https://doi.org/10.1038/cdd.2014.195.
[50] M. Glei, S. Klenow, J. Sauer, U. Wegewitz, K. Richter, B.L. Pool-Zobel, Hemoglobin and hemin induce DNA damage in human colon tumor cells HT29 clone 19A and in primary human colonocytes, Mutat. Res. 594 (2006) 162–171, https://doi.org/10.1016/j.mrfmmm.2005.08.006.
[51] C. Gemelli, B.M. Dongmo, F. Ferrarini, A. Grande, L. Corsi, Cytotoxic effect of hemin

in colonic epithelial cell line: involvement of 18 kDa translocator protein (TSPO), Life Sci. 107 (2014) 14–20, https://doi.org/10.1016/j.lfs.2014.04.026.
[52] M.K. Nayak, P.P. Kulkarni, D. Dash, Regulatory role of proteasome in determination of platelet life span, J. Biol. Chem. 288 (2013) 6826–6834, https://doi.org/10.1074/jbc.M112.403154.
[53] M.K. Nayak, K. Kumar, D. Dash, Regulation of proteasome activity in activated human platelets, Cell Calcium 49 (2011) 226–232, https://doi.org/10.1016/j.ceca.2011.02.005.
[54] E.D. Hottz, A.P.T. Monteiro, F.A. Bozza, P.T. Bozza, Inflammasome in platelets: allying coagulation and inflammation in infectious and sterile diseases? Mediat. Inflamm. 2015 (2015) 435783, , https://doi.org/10.1155/2015/435783.
[55] M. Paul, K. Kemparaju, K.S. Girish, Inhibition of constitutive NF-κB activity induces platelet apoptosis via ER stress, Biochem. Biophys. Res. Commun. 493 (2017) 1471–1477, https://doi.org/10.1016/j.bbrc.2017.10.011.
[56] E.D. Hottz, J.F. Lopes, C. Freitas, R. Valls-de-Souza, M.F. Oliveira, M.T. Bozza, A.T. Da Poian, A.S. Weyrich, G.A. Zimmerman, F.A. Bozza, P.T. Bozza, Platelets mediate increased endothelium permeability in dengue through NLRP3-inflammasome activation, Blood. 122 (2013) 3405–3414, https://doi.org/10.1182/blood-2013-05-504449.
[57] R.K.A. Sayed, M. Fernández-Ortiz, M.E. Diaz-Casado, P. Aranda-Martínez, J. Fernández-Martínez, A. Guerra-Librero, G. Escames, L.C. López, R.M. Alsaadawy, D. Acuña Castroviejo, Lack of NLRP3 inflammasome activation reduces age-dependent sarcopenia and mitochondrial dysfunction, favoring the prophylactic effect of melatonin, J. Gerontol. A Biol. Sci. Med. Sci. 14 (2019), https://doi.org/10.1093/gerona/glz079 pii: glz079.